Open Access Journal

Journal of Sustainable Research in Engineering Vol. 3 (3) 2016, 74-81

Journal homepage: http://sri.jkuat.ac.ke/ojs/index.php/sri

Development of a Fault Location and Identification System for Underground Transmission Cables Based on Wavelet-ANFIS Method

Hastings. S. Zawaira[1*], George. N. Nyakoe[2], Christopher M. Muriithi[3]

[1]*Department of Electrical Engineering, power option, Pan African University, Institute for Basic Sciences, Technology and Innovations, Kenya*

[2]*Department of Mechatronic Engineering, Jomo Kenyatta University of Agriculture and Technology P. O. Box 62000-00200, Nairobi, Kenya.*

[3] *Department of Electrical & Power Engineering, Technical University of Kenya, Nairobi, Kenya*

**Corresponding Author - hszawaira@yahoo.com*

Abstract Transmission lines are the backbone of electrical power systems and other power utilities as they are used for transmission and distribution of power. Power is distributed to the end user through either overhead cables or underground cables. In the case of underground cables, their propensity to fail in service increases as they age with time. The increase in failure rates and system breakdowns on older underground power cables are now adversely impacting system reliability and many losses involved; therefore, it is readily apparent that necessary action has to be taken to manage the consequences of this trend. At any given length of a cable, its deterioration or indication of failure manifests itself through discrete defects. Identification of the type of defects and their locations along the length of the cables is vital in order to minimize the operating costs by reducing lengthy and expensive patrols to locate the faults, and to speed up repairs and restoration of power in the lines. In this paper, a method that combines wavelets and neuro-fuzzy technique for fault location and identification is proposed. A 100km, 220KV, 50Hz power transmission line model was developed and different faults and locations simulated in MATLAB/SIMULINK, and then certain selected features of the wavelet transformed signals were used as inputs for training and development of the Adaptive Network Fuzzy Inference System (ANFIS). The results obtained from ANFIS output were compared with the raw values. Comparison of the ANFIS output values and the actual values shows that the percentage error was established to be less than 2.5%. Thus, it can be concluded that the wavelet-ANFIS technique is accurate enough to be used in identifying and locating underground power line faults.

Keywords ANFIS, Discrete Wavelet Transform (DWT), Fault location, Fault types, and Underground cables.

1. Introduction

In electrical power systems, transmission and distribution lines are pivotal links that accomplish the continuity of service from the generating plants to the end users. Electrical power can be distributed to the end user through either over-head cables or underground cables. The main goal of the connections is to provide power in a very safe, reliable and affordable way to the end user. Underground power cables have been widely implemented and favoured due to their reliability and limited environmental concerns. These underground cable systems are manufactured to have a long life with reliability. However, the useful life span of these cables is not infinite [1]. Mashikian and Szatkowski, [2] highlighted that as these underground cables age, their propensity to fail in service increases, thus at any given length of a cable, its deterioration or indications of failure manifests itself through discrete defects.

Due to the increasing failure rates and system breakdowns affecting underground power cables, a fast and accurate fault detection method is essential to hasten system restoration, reduce outage time and minimize financial loses [3]. Complete replacement of old or failing cable system is not an option since cable systems do not age uniformly. To improve the reliability of a transmission system, accurate fault location and identification is required in order to reduce the fault time interruptions, improve system reliability and ensure customer satisfaction. Conventionally, methods that have been used for identifying and locating the cable defects, were time consuming and inefficient. This led to the introduction of better techniques of fault identification such as Time Domain Reflectometer (TDR), wavelet and artificial intelligence based methods [4].

Ningkang and Yuan [5] introduced a mathematical model that calculates the impedance across a tested transmission line to confine all fault locations. They used only the post-fault phase magnitude current to identify fault location. This was however satisfactory but the method is not appropriate for distribution system due to asymmetrical network. Another method which provided an alternative to identify fault location for a radial cable is presented in [6]. The method uses wavelet transform to extract valuable information from transient signals and eventually localize faults through a fuzzy logic system. Javad [7] implemented another approach to locate faults in a combined overhead transmission line with underground power cable using ANFIS. This scheme consists on training the ANFIS system with a fault database registers. The database was obtained from the power distribution system. The overall performance of the system was good, and 99.14% of the current patterns were correctly classified.

This paper builds upon previously presented methods to design a fast and accurate method that can identify and locate faults in an underground power cable. The proposed method uses wavelet-ANFIS combined approach. In the next section, a theoretical summary of the transmission line model is presented. In the subsequent sections, the development of the transmission line simulation model, design of the wavelet-ANFIS and, simulation results and their discussion are presented.

2. Theoretical Model of Transmission Line

The solution for a uniform transmission line which has losses can be obtained with the equivalent circuit for the elementary cell shown in Figure 1.

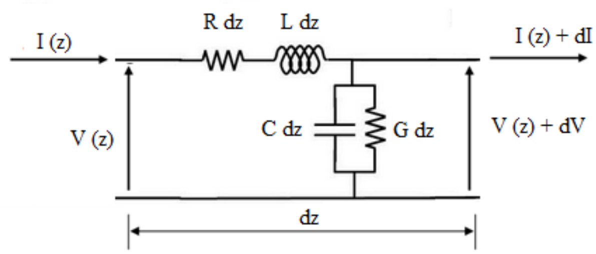

Fig.1. Section of a transmission line

The series impedance of the circuit in Figure 1 determines the variation of the voltage from the sending end, input to the receiving end, and the output of the cell. The corresponding equation for the series impedance of the circuit is:

$$(V + dv) - V = -(j\omega L dz + R dz)I \tag{1}$$

From the above equation, we can obtain a first order differential equation for the voltage as follows:

$$\frac{dv}{dz} = -(j\omega L + R)I \tag{2}$$

The current flowing through the shunt admittance determines the input-output variation of the current and the corresponding circuit equation is:

$$dI = -(j\omega C dz + G dz)(V + dV) \tag{3}$$

$$dI = -(j\omega C + G)dz - (j\omega C + G)dvdz \tag{4}$$

Using Equation (4), a first order differential equation for the current will be:

$$\frac{dI}{dz} = -(j\omega C + G)V \tag{5}$$

Equations (2) and (5) describe the behaviour of voltage and current on the lossy transmission line. These two equations are referred to as the “telegraphers’ equations” for the lossy transmission line. To obtain a set of uncoupled equations, Equations (2) and (5) are differentiated with respect to the coordinate ***z***, to produce the “telephonists’ equations” for the lossy line. These telephonists’ equations for the transmission line are uncoupled second order differential equations and they are also wave equations. The wave propagation constant which is a complex quantity is:

$$\gamma = \sqrt{(j\omega L + R)(j\omega C + G)} = \alpha + j\beta \tag{6}$$

From Equation (6), the real part α of the propagation constant γ describes the attenuation of the signal due to resistive losses and the imaginary part β describes the propagation properties of the signal waves in loss-less lines. The exponential terms including α are the real parts, therefore, they only affect the magnitude of the voltage phasor. The exponential terms including β have unitary magnitude and are purely imaginary argument, so they affect only the phase of the waves in space. The current distribution for the transmission line can be obtained by differentiating the result of the voltage as follows:

$$I(z) = \sqrt{\frac{(j\omega C + G)}{(j\omega L + R)}}(V^{+}e^{-\gamma z} - V^{-e^{\gamma z}})$$

$$= \frac{1}{Z_0}(V^{+}e^{-\gamma z} - V^{-}e^{\gamma z}) \quad (7)$$

The characteristic impedance of the transmission line is given by:

$$Z_0 = \sqrt{\frac{(j\omega C+G)}{(j\omega L+R)}} \quad (8)$$

The characteristic impedance of the line in Equation (8) is applicable for both loss-less and lossy transmission lines. This characteristic impedance does not depend on the line length, but only on the material of the conductors, the dielectric material surrounding the conductors and the geometry of the line cross section, which determine the parameters *L*, *R*, *C*, and *G*.

3. Transmission Line Simulation Model and Fault Identification

The development of the transmission line was done under MATLAB/SIMULINK environment. The line considered is a 100km, 220KV, 50Hz underground power cable. The system analyzed post fault conditions and all the simulations done were to generate fault signals to be used to identify and locate the faults and generate a database for later use. The fault is created after every 5km distance, with a simulation time of 0.001s, sample time = 0, resistance per unit length = 0.012Ω, inductance per unit length = 0.9 mH and capacitance per unit length = 127µF. The system considers a constant load and the phase angle is also varied between -120° to 120°, with the increasing step of 30°, phase A being the reference. Phase angle was used because it was indicating some variations on the fault location when initial simulations were carried out. Figure 2 shows the line model which was developed.

3.1 Fault Identification Approach

The transmission line model system was simulated to identify the type of fault on the affected phase. The system was designed with a means of observing all the phases on the transmission line on one platform, using the scope in MATLAB/SIMULINK.

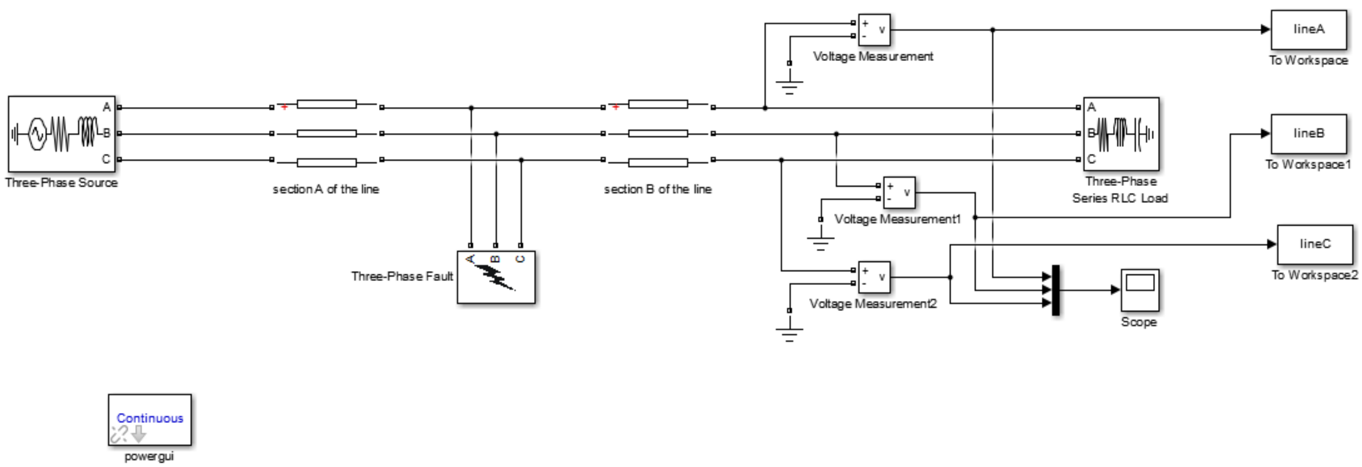

Fig. 2. Line model

On the scope, all transmission line wave forms were observed and the line which has been affected shows a deviation from the normal expected waveforms. The fault data from the toolbox on the line was used to locate the fault. To distinguish the faults, different wave forms were observed. For a single line fault, only one phase had a lower magnitude of voltage as compared to the other two. In a double phase fault, two of the signals with faults indicated some deviations from the expected wave form. When the type of the fault had been established, fault data, which can be referred to as signal ***s*** from the line was analyzed under wavelet transform to extract useful information pertaining to the fault.

4 Fault Location using Discrete Wavelet Analysis

To enable fault location along the transmission line, the initial stage is to analyze the fault signals so as to identify the affected phase(s). Simulated line data from the affected phase is transferred to Discrete Wavelet Analysis in MATLAB/SIMULINK environment for data processing and analysis. To accomplish the task, features of the line voltage signals are extracted based on discrete wavelet transform with daubechies5 (db5) as the mother wavelet. The feature extracted from the line is an index representing the location of the fault, represented by spikes on the DWT. Analysing signal ***s*** under discrete wavelet analysis, involves passing the signal through a number of filters. Firstly the sample signal ***s*** is passed through a low pass filter which has an impulse response g resulting in a convolution of the two.

$$s[n] = (x * g)[n] = \sum_{k=-\infty}^{\infty} x[k]g[n-k] \qquad (9)$$

After the signal has passed through a low pass filter, it is further decomposed simultaneously using a high pass filter ***h***. Both outputs from the high pass filter and low pass filter, produce~~s~~ detail coefficients and approximation coefficients respectively. The two filters are related to one another and they are referred to as the quadrature mirror filters. Figure 3 represents the combined scheme of the filters and the expected coefficient outcome.

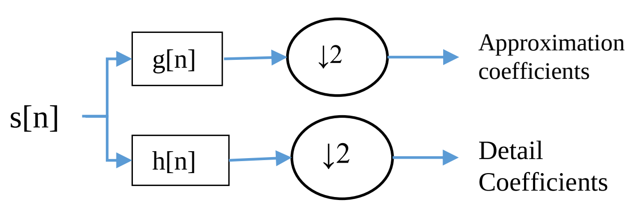

Fig. 3. High pass and low pass signal filtering

Since half the frequencies of the signal have now been removed, according to Nyquist's rule, half the samples can be discarded. Equations (10) and (11) represent the two new coefficients of the initial signal.

$$y_{low}[n] = \sum_{k=-\infty}^{\infty} x[k]h[2n-k] \qquad (10)$$

$$y_{high}[n] = \sum_{k=-\infty}^{\infty} x[k]g[2n-k] \qquad (11)$$

After the first decomposition, the signal will have halved the time resolution since only half of each filter output characterises the signal. The two outputs each have half the frequency band of the input so the frequency resolution has been doubled. Depending with the level to which the signal has to be analysed, the process of passing the new signal over the low pass and high pass filter will continue until the level of analysis has been achieved. The summation of the two equations can be written more concisely as:

$$y_{low} = (x * g) \downarrow 2 \qquad (12)$$

$$y_{high} = (x * h) \downarrow 2 \qquad (13)$$

To further increase the frequency resolution of the signal and the approximation coefficients decomposed with the high pass and low pass filters, the decomposition process is repeated a number of times and then down-sampled. This can be represented as a binary tree known as a filter bank with nodes representing a sub-space of different time-frequency localisation.

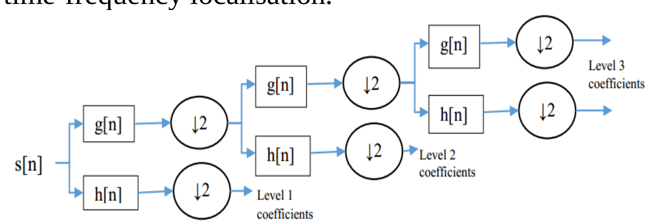

Fig. 4. Signal decomposition

At each level in Figure 4, the signal is decomposed into low and high frequencies. Because of the decomposition process, the input signal must be a multiple of 2^n where n represents the number of levels. The filter bank implementation of wavelets in general can be interpreted as computing the wavelet coefficients of a discrete child wavelets from a given mother wavelet ψ(t). In this case, the mother wavelet is shifted and scaled by powers of two as shown be equation (14).

$$\psi_{j,k}(t) = \frac{1}{\sqrt{2^j}}\psi\left(\frac{t-k2^j}{2^j}\right) \qquad (14)$$

where j {\displaystyle j} j is the scale parameter and k {\displaystyle k} k is the shift parameter. Signal S will be analysed up to level 5. When a signal passes through a fault on the transmission line, the signal will experience a disturbance. By analysing the signal under wavelet transform, the signal will be broken down into shifted and scaled versions of the original wavelet to obtain a better resolution of the disturbance.

5. ANFIS Model for Fault Location

Database created after wavelet analysis for different faults and locations was used as the input in the training of the ANFIS. In designing the model, the inputs were matched to the outputs and the system was trained to look for a relationship between the inputs and the output. When testing, the system is to estimate the correct output, based on the set of inputs provided to the system. Figure 5 shows the overall ANFIS model which was developed.

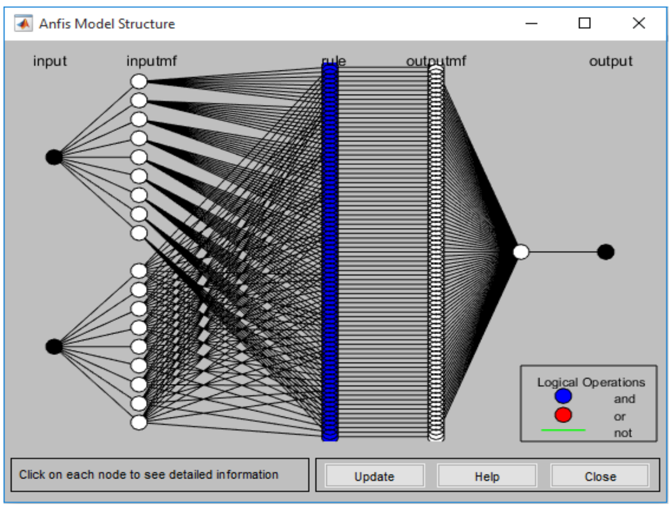

Fig. 5. ANFIS model structure

5.1 ANFIS Inference Engine

The ANFIS has a dual-input and single output. The inputs of the ANFIS are phase angle and index. The universe of discourse for the phase angle was normalized to cover a range of [-120, 120] and for the index to cover a range of [18, 2144]. A choice of nine membership functions for the two fuzzy variables was chosen, (meaning 81 rules in the rule base). These rules were generated automatically by the ANFIS since it used the black box to train the system. The resulting rule base is shown in the Table 1.

Table 1: Rule base for the ANFIS

PHASE ANGLE	INDEX								
	UH	MH	LH	H	M	L	LL	ML	UL
ENL	MF 1	MF 2	MF 3	MF 4	MF 5	MF 6	MF 7	MF 8	MF 9
LGN	MF 10	MF 11	MF 12	MF 13	MF 14	MF 15	MF 16	MF 17	MF 18
MN	MF 19	MF 20	MF 21	MF 22	MF 23	MF 24	MF 25	MF 26	MF 27
LN	MF 28	MF 29	MF 30	MF 31	MF 32	MF 33	MF 34	MF 35	MF 36
Z	MF 37	MF 38	MF 39	MF 40	MF 41	MF 42	MF 43	MF 44	MF 45
LP	MF 46	MF 47	MF 48	MF 49	MF 50	MF 51	MF 52	MF 53	MF 54
MP	MF 55	MF 56	MF 57	MF 58	MF 59	MF 60	MF 61	MF 62	MF 63
LGP	MF 64	MF 65	MF 66	MF 67	MF 68	MF 69	MF 70	MF 71	MF 72
ELP	MF 73	MF 74	MF 75	MF 76	MF 77	MF 78	MF 79	MF 80	MF 81

The rules can be read as shown below:

1. If (phase_angle is ENL) and (fault_index is UH) then (distance_(Km) is MF1)
2. If (phase_angle is ENL) and (fault_index is MH) then (distance_(Km) is MF2)
3. If (phase_angle is ENL) and (fault_index is LH) then (distance_(Km) is MF3)

6. Results and Discussion

To identify the phase which has been affected, the system was designed to print out all the phases and their behaviour.

6.1 Single phase fault

Figure 6 represents three-phase voltage signals for Line A, Line B and Line C and their detail coefficients at single phase fault condition. From this figure, it can be observed that Line A was affected because of the change in the amplitude and the two spikes appearing. The amplitude of Line A has been reduced and the fault in line A affects the other lines. This can be observed by the small differences observed on line B and Line C. Because the system initially was a balanced three phase system, when one of the lines is affected, it causes interference with the other line. The straight line displayed by the entire signal represents the initiation time for the simulation. The spike appearing at the beginning of the signal represents the current initiation stage in the transmission line. The second spike indicates the fault location. The fault appears on the system at a specific time which after wavelet analysis shows the location of the fault. Once the fault has been identified, fault data is transferred to wavelet analysis for fault location.

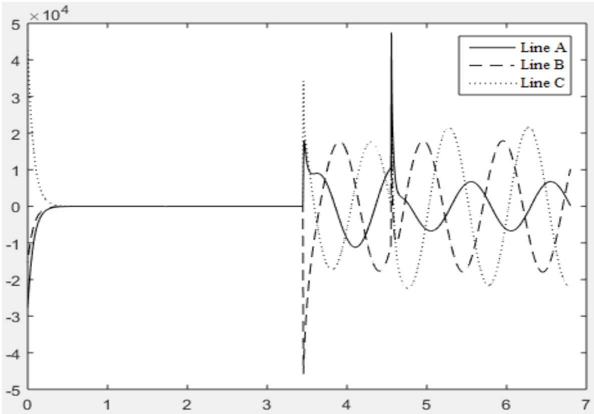

Fig. 6. Fault identification for single phase fault

6.2 Discrete Wavelet Transformation

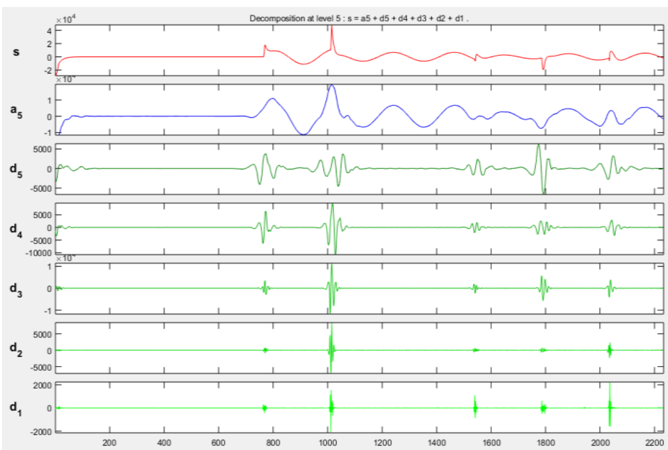

Fig. 7. Wavelet transformation

In Figure 7, the signal has been analysed up to level 5, indicated by $d_1 - d_5$. The nature of the plot of detailed coefficients at level 1 reveals a sharp spike which corresponds to the fault initiation process. According to DWT theory, the spikes represent the highest frequency within the fault signal, but it is also however, not practical to identify a fault based on these spike only since such spikes will occur every time there is a sudden change in the cable current signal. So for precise fault location, all the levels were observed to identify consistence of spike location on all the levels. Under wavelet analysis, the location appeared as an index or number as a result of the partitions within the toolbox, instead of the time variable. The index was used in ANFIS to identify the location of the fault. The ANFIS was developed in such a way that it makes use of the wavelet index and the phase angle of the transmission line to locate the fault. Figure 8 shows the graphic user interface for the ANFIS fault location system.

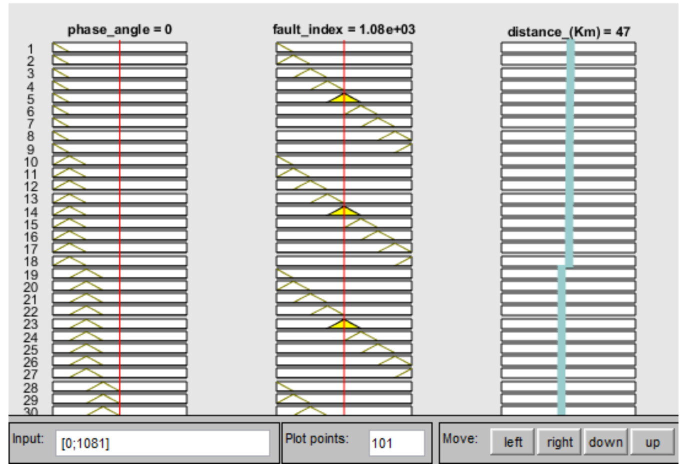

Fig. 8. ANFIS GUI

To test the efficiency and establish the accuracy of the system, a number of simulations had to be done and identify how the system will perform. Using Equation (15) to identify the accuracy of the system, Table 2 is showing the results of the simulations done at random fault locations selected on the line to establish the accuracy of the ANFIS.

$$\%Error = \frac{(Actual\ fault\ location - Calculated\ fault\ location)}{total\ faulty\ section\ length}\ x\ 100 \qquad (15)$$

Basing on the simulations done, the % error of the system is in the range of -1.1 to 2.2%, and the average being = 0.0235%

Table 2: Test values and error estimation

Actual Distance (Km)	Calculated Distance (Km)	Difference	% error
4.5	4.4	0.1	2.22
9.4	9.5	-0.1	-1.06
13.3	13.3	0	0
18.2	18.4	-0.2	-1.10
22.1	22.0	0.1	0.45
28.4	28.6	-0.2	-0.70
34.7	34.7	0	0
36.9	36.8	0.1	0.27
41.0	40.8	0.2	0.49
47.2	47.1	0.1	0.21
50.6	50.6	0	0
59.1	59.1	0	0
62.0	62.2	-0.2	-0.32
67.5	67.4	0.1	0.15
71.9	72	-0.1	-0.14
76.8	76.8	0	0
83.0	83.0	0	0
85.6	85.6	0	0
92.8	92.8	0	0
96.9	96.9	0	0
Average			**0.0235**

From Table 2, it can be observed that the general difference between the simulated values and the actual fault locations are around 0.2 or 0.1. If expressed as a percentage error from a specific line segment as shown in Figure 9, in other sections, the percentage error is big. The system was generally accurate across different segments of the line as shown in Figure 9 with the bottom 50km from the sending end constituting most of the errors as compared to the upper region. On distances less than 50km, after wavelet analysis the index had a greater margin between the two consecutive test values as compared to distances greater than 50km. This difference when developing the ANFIS will leave faults below 50km to have a bigger risk of errors when testing the system. The bigger difference between the two margins was from the partitions within the wavelet tool box used, which cannot be changed. Basing on the test values, the system is accurate enough to be used for fault location and identification.

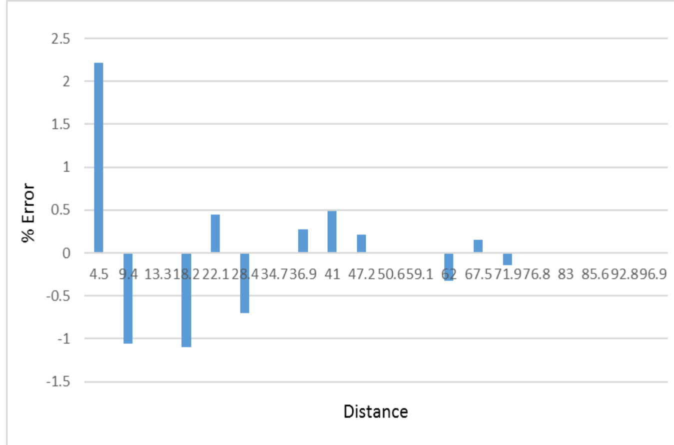

Fig. 9. Distance and % error graph

7. Conclusions

The application of the discrete wavelet transform and ANFIS to identify and estimate the fault location on transmission line has been investigated. The most suitable wavelet family was made to identify fault type and estimate the fault location on the transmission line. It was found that better results were achieved using Daubechies ‘db5’ wavelet with an error of less than 2.5%. Simulations for the 220kv, 100km transmission line were performed using SIMULINK/ MATLAB software. It was shown that the proposed method for fault location and identification system for underground power cables based on wavelet-ANFIS technique is accurate enough to be used in detection of transmission line fault. Further research was recommended to focus more on how the faults development and how they affect the system so that a predictive fault location system can be developed to help the power utility and the consumers manage the use of their equipment and reduces losses to both parties.

References

[1] M. Mashikian, A. Szatkowski,” Medium Voltage Cable Defects Revealed by Off-LinePartial Discharge Testing at Power Frequency”, *IEEE Electrical Insulation Magazine*, Vol. 22, No. 4, p. 24-32–July/August 2006.

[2] Magdy B. Eteiba, Wael Ismael Wahba, Shimaa Barakat, “ANFIS Approach for Locating Faults in Underground Cables”, *World Academy of Science, Engineering and Technology International Journal of Electrical, Computer, Energetic, Electronic and Communication Engineering* Vol:8, No:6, 2014.

[3] Jorge Altamirano, Tim Andrews, Miroslav Begovic, Yamille del Valle, Ron Harley, J. C. Hernandez Mejia, Thomas J. Parker. Diagnostic testing of underground cable systems (cable diagnostic focused initiative) *NEETRAC project numbers*: 04-211/04-212/09-166, December 2010

[4] Amir Tabatabaei, Mohammad-Reza Mosavi, Abdolreza Rahmati, "Fault Location Techniques in Power System based on Traveling Wave using Wavelet Analysis and GPS Timing," *Przegląd Elektrotechniczny*, vol. 88, no. 6, pp. 347 - 350, 2012.

[5] Ningkang and Yuan Liao, Fault Location Estimation Using Current Magnitude Measurements, *Proceedings of the IEEE Southest Conference (SECON 10)*, 2010.

[6] J. Moshtagh, R. K. Aggarwal , A new approach to fault location in a single core underground cable system using combined fuzzy logic & wavelet analysis, *The Eight IEE International Conference on Developments In Power System Protection*, pp. 228 231, April 2004.

[7] Javad Sadeh, Hamid Afradi , A new and accurate fault location algorithm for combined transmission lines using Adaptive Network-Based Fuzzy Inference System , *Electric Power Systems Research* vol. 79, pp. 1538–1545, (2009).

[8] J. J. Mora, G. Carrillo , Fault Location in Power Distribution Systems using ANFIS Nets and Current Patterns, *IEEE PES Transmission and Distribution Conference and Exposition* Latin America, Venezuela, 2006.

[9] Magdy B. Eteiba, Wael Ismael Wahba, Shimaa Barakat, "Accurate fault location algorithm for Underground Cables using Adaptive Network Based Fuzzy Inference System and Discrete Wavelet Transform," *IPASJ International Journal of Electrical Engineering (IIJEE)*, vol. 2, no. 5, pp. 1 - 11, May 2014.